JOURNAL OF Materials CHEMISTRY

Effect of H_2 addition on SiCN film growth in an electron cyclotron resonance plasma chemical vapor deposition reactor

Jih-Jen Wu,[a] Kuei-Hsien Chen,[a] Cheng-Yen Wen,[b] Li-Chyong Chen,[b] Juen-Kai Wang,[b] Yueh-Chung Yu,[c] Chang-Wan Wang[c] and Erh-Kang Lin[c]

[a]*Institute of Atomic and Molecular Sciences, Academia Sinica, Taipei, Taiwan. E-mail: jjwu@pub.iams.sinica.edu.tw*
[b]*Center for Condensed Matter Sciences, National Taiwan University, Taipei, Taiwan*
[c]*Institute of Physics, Academia Sinica, Taipei, Taiwan*

Received 26th October 1999, Accepted 4th January 2000

The effect of H_2 addition on SiCN film growth was studied in an electron cyclotron resonance plasma chemical vapor deposition reactor. No carbon incorporation was observed in the film by feeding $CH_4/SiH_4/N_2$ even at $CH_4:SiH_4$ ratios as high as 150:1. With H_2 addition and at a $CH_4:SiH_4$ ratio of 100:1 and above, the carbon contents within the films increased significantly. Possible explanations for this behavior involve gas phase and surface reactions of hydrogen including formation of active carbon species in the gas phase by hydrogen abstraction reactions and preferential etching of surface-bonded carbons.

1 Introduction

The synthesis of ternary Si–C–N systems has been of growing interest in recent years. Several methods have been developed to produce Si–C–N films and powders.[1–11] Amorphous SiCN films have been deposited by pulsed laser ablation and electron cyclotron resonance (ECR) plasma CVD.[1,2] Amorphous SiCN nano-powders produced by laser and RF discharges have also been reported.[3,4] Riedel *et al.*[5] adopted polyorganosilylcarbodiimides as precursor materials and have successfully synthesized nanocrystalline Si_2CN_4. We have demonstrated that large ($\approx\mu m$) silicon carbon nitride crystals with a wide range of composition are deposited by microwave CVD.[6–9] Optical investigation of these crystals further indicates the potential of the ternary SiCN compound for blue and UV optoelectronic applications.[9] Badzian *et al.*[10] also reported that crystalline silicon carbonitride grown by microwave plasma CVD may have some physical properties that can compete with those of c-BN.

In previous work[11] we reported that continuous polycrystalline silicon carbon nitride films have been successfully deposited by ECR plasma chemical vapor deposition. The ECR plasma CVD process significantly enhanced the nucleation density up to 10^{11} cm^{-2} which is 4 orders of magnitudes higher than those deposited by microwave plasma CVD (MWCVD) alone.[9] Typical (Si; C) to N composition ratios of the films thus deposited were around 0.75:1, which is identical to the theoretical value for Si_3N_4.

Hydrogen atoms are known to be crucial in facilitating deposition of metastable diamond phase by maintaining the sp^3 structure of carbon atoms on the substrate surface, abstracting hydrogen atoms from surface bonded C–H, preferentially etching the graphitic phase of carbon, and initiating free-radical reactions in the gas phase.[12] However, the effect of hydrogen atoms in the growth of crystalline carbon nitride, which is also predicted to be a metastable covalent material, has not been addressed. For the growth of crystalline β-C_3N_4, the sp^3 structure of the carbon atoms and the sp^3 C–N bonding configurations must also be maintained. The fact that crystalline carbon nitride films can be deposited under hydrogen-free environments (such as in most sputtering processes) or hydrogen environments (such as various CVD using either $CH_4/NH_3/H_2$[13] or CH_4/N_2[14] gas) makes the role of hydrogen in the growth process quite obscure. It is not certain whether hydrogen atoms are needed in stabilizing the sp^3 structure of C atoms during growth of CN. To study the roles of hydrogen in the growth of SiCN films, we examine the effect of H_2 addition on the compositions and structures of films deposited at various CH_4 to SiH_4 ratios in the feed. Optical emission spectroscopy (OES) was employed to monitor *in situ* the fluorescing species in the gas phase. Rutherford backscattering spectroscopy (RBS), X-ray photoelectron spectroscopy (XPS), and Transmission Electron Microscopy (TEM) with X-ray Energy Dispersive Spectrometry (XEDS) were employed to characterize the composition, the bonding, and the structure of the films.

2 Experimental

A schematic of the ECR plasma system employed in this study is shown in Fig. 1. The ECR plasma CVD system consists of a 20 cm diameter ECR chamber and a 40 cm diameter process

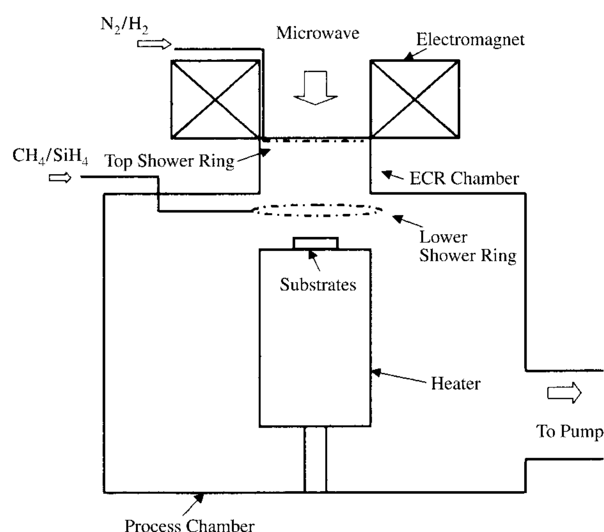

Fig. 1 A schematic diagram of the electron cyclotron resonance plasma chemical vapor deposition reactor.

This journal is © The Royal Society of Chemistry 2000

chamber equipped with a substrate stage in which a BN heater is used for independent control of the substrate temperature. A thermocouple placed underneath the substrate holder was used to monitor the temperature of the holder. A 1.5 kW Astex AX2115 microwave source and an AX4400 electromagnet were employed to generate the ECR plasma as nitrogen or hydrogen was introduced into the ECR chamber of the reactor from the top shower ring, right below the quartz window. To avoid coating on the quartz window, CH_4 and SiH_4 were fed into the process chamber far away from the ECR absorption zone through the lower shower ring just above the substrate holder. The base pressure of the reactor was 1×10^{-6} Torr evacuated by a turbo molecular pump. Pre-cleaning of silicon substrates was performed by H_2 ECR plasma before deposition. In order to study the roles of hydrogen, film growth characteristics were compared for various CH_4 : SiH_4 ratios with and without H_2 addition at a constant substrate temperature of 1023 K, reactor pressure of 3.2 mTorr, and microwave power of 700 W.

Quantitative composition analyses of the films were performed by RBS. High energy ^{4}He ion beams of 3.5 MeV with a fixed scattering angle of 165° were employed to increase the sensitivity of N and C elements.[15,16] The non-RBS cross sections of ^{4}He ion from C and N[15,16] were linked to the RUMP2 program (ver. 3.512, 1993) for RBS data analysis. Standard SiC and Si_3N_4 films were used to calibrate the RBS measurement. A Perkin-Elmer Phi 1600 electron spectroscopy for chemical analysis (ESCA) system was used to study the chemical bonding state of the films. Mg-Kα radiation of 1253.6 eV was used as the X-ray source with a linewidth of 0.7 eV. The analysis area for XPS measurement was 800 μm diameter and the pass energy for the chemical state analysis was 11.75 eV. The structures of the films were studied by using a JEOL 2010 transmission electron microscope. Optical emission, in the range of 350–800 nm, from the ECR plasma was monitored through a quartz viewport and an optical fiber. The OES system consisted of an ARC SpectraPro-500 grating monochromator with 1200 grooves mm^{-1} and a Hamamatsu R955 photomultiplier detector.

3 Results and discussion

3.1 Composition, bonding and structure of deposited films

Quantitative analyses of RBS data for the compositions of a series of films deposited with or without H_2 addition are listed in Table 1. As shown only silicon nitride film was formed without H_2 addition during growth. Considering that the C : Si ratio in the gaseous precursor ranged from 62.5 to 150 : 1, it is somewhat surprising that there was no carbon detected in the film. In the case of H_2 addition, carbon still did not appear in the RBS spectrum of film deposited at a CH_4 : SiH_4 ratio of 83.3 : 1 and below. At higher ratios, however, the carbon content increased significantly. The RBS spectra of the films deposited with or without H_2 addition at CH_4 : SiH_4 ratios of 62.5 and 100 : 1 are shown in Fig. 2. The results indicated that,

Table 1 The composition of the films deposited at various CH_4 to SiH_4 ratios (R) with or without H_2 addition

Sample no.	Reactant flow rate/cm^3 s^{-1} H_2	$N_2/CH_4/SiH_4$	R	Film composition N/C/Si
ECR50	0	5/1.25/0.02	62.5	63/0/37
ECR55		5/1.25/0.015	83.3	62/0/38
ECR54		5/1.5/0.015	100	63/0/37
ECR66		5/2.25/0.015	150	59/0/41
ECR48	2.5	2.5/1.25/0.02	62.5	61/0/39
ECR64		2.5/1.25/0.015	83.3	59/0/41
ECR62		2.5/1.5/0.015	100	61/18/21
ECR67		2.5/2.25/0.015	150	59/20/21

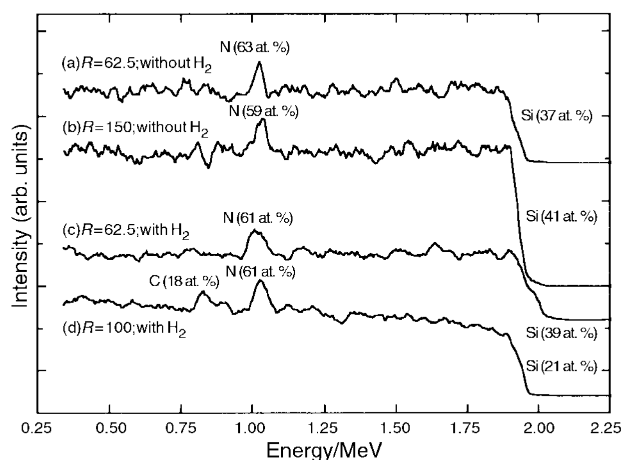

Fig. 2 RBS spectra of the films deposited with and without H_2 additions at CH_4 : SiH_4 ratios of 62.5 and 100 : 1.

at sufficient methane concentrations, H_2 addition promoted carbon incorporation in the SiCN films in the ECR plasma CVD process.

Typical high resolution XPS scans of Si(2p), C(1s), and N(1s) peaks of the SiCN film are shown in Fig. 3. It reveals that the peaks were composed of more than one Gaussian peak. The C(1s) photoelectron peak is composed of three components centered at 284.0, 285.3, and 287.4 eV, whereas the N(1s) peak also consists of two components centered at 398.0 and 398.8 eV. According to the tentative assignment by Marton *et al.*,[17] these peaks correspond to C–C, C(1s)=N, C(1s)–N; and N(1s)–Si and N(1s)–C, respectively. The Si(2p) photoelectron peak was resolved into two peaks centered at 102.2 and 104.0 eV, which were assigned to Si(2p)–N and Si(2p)–O bonding, respectively. The C–C peak at 284.0 eV and Si–O peak at 104.0 eV disappeared after sputtering with Ar^+ ions,

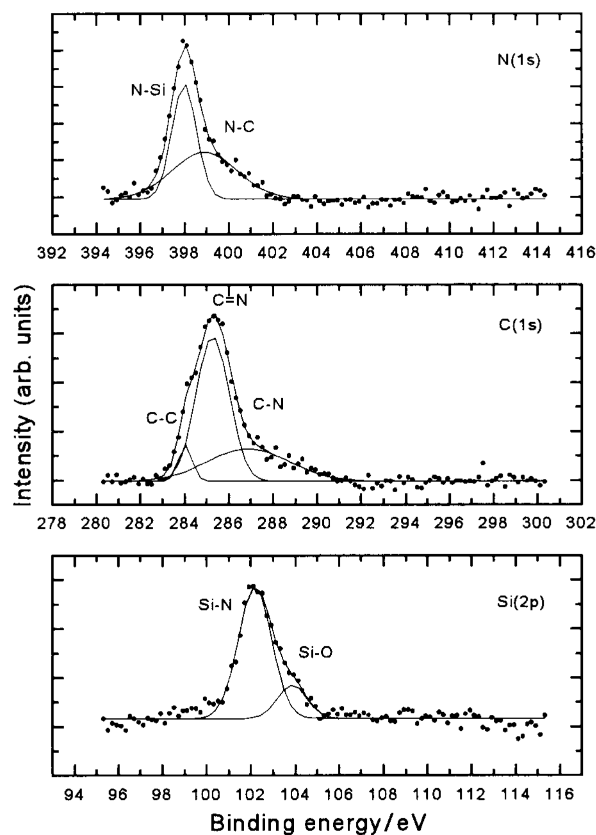

Fig. 3 XPS spectra of C(1s), N(1s) and Si(2p) of the SiCN film deposited with H_2 addition.

indicating that C–C and Si–O bondings were due to surface contamination. There is no detectable C(1s)–Si bonding signal at 282.8 eV, which is also confirmed by the absence of a Si(2p)–C signal around 100.3 eV, indicating that Si–C bonds in the film are negligible.

Transmission Electron Microscopy was employed to investigate the microstructure of the SiCN film. The TEM image and selected area diffraction (SAD) pattern of the SiCN film are shown in Fig. 4. Fig. 4(a) shows that the SiCN film is composed of nanocrystals embedded in the amorphous phase. The carbon content in amorphous as well as nanocrystalline phases was found to be almost the same by XEDS. The *d* spacings of the nanocrystals observed from the SAD pattern, internally calibrated by the SAD pattern of Si(100) substrate, are listed in the Table 2. The *d* spacings of the SiCN film were within 6% of those for α-Si_3N_4. Preliminary estimates of the magnitudes of lattice parameters *a* and *c* (as conventionally defined for hexagonal structure) are 0.79 and 0.60 nm, respectively. Si–C bonds in the film are negligible as indicated by XPS analyses, implying that C substitutes only for the Si sites in the α-Si_3N_4 structure so that C and Si are always "bridged" by nitrogen in the SiCN film. Hence, the SiCN crystal can be seen as being built from zigzag chains of Si–C–N atoms. Badzian *et al.* proposed that carbon substitution might cause linear disorder of these chains[10] and lead to the disappearance or discrepancy in the intensity of certain reflections. In our case the carbon content is around 20 at.% (*i.e.*, C : Si ratio is about 1 : 1), whereas the SiCN film reported by Badzian *et al.* contains only a few to 6 at.% of C.[10] More substantial discrepancies between our SiCN film and α-Si_3N_4, shown in Table 2, could result from the higher linear disorder of atoms by a larger fraction of the carbon substitution in our case than those reported by Badzian

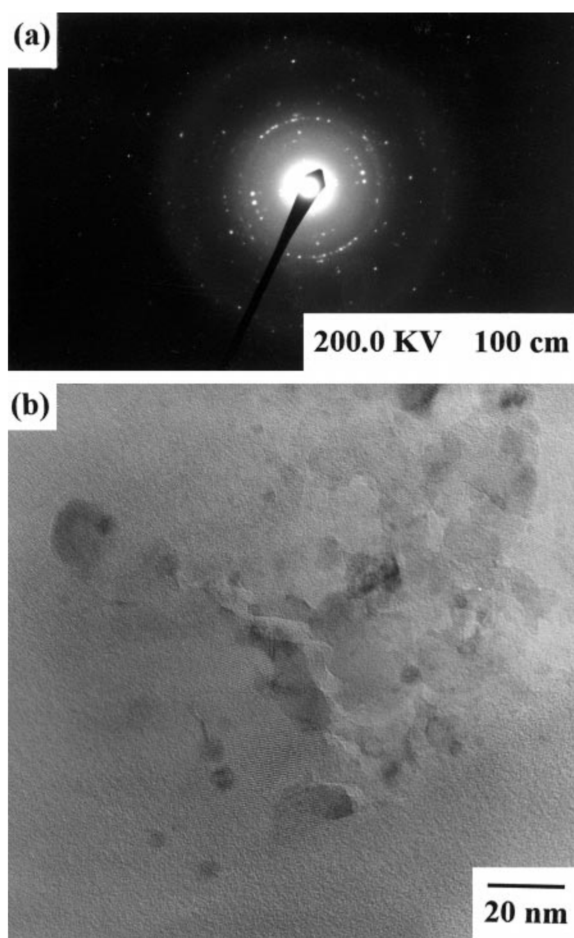

Fig. 4 (a) The SAD pattern of the SiCN film. (b) The HRTEM image of the SiCN film.

Table 2 Comparison of the *d* spacings determined experimentally from transmission electron diffraction of Fig. 4(b) with those of α-Si_3N_4

Measured		α-Si_3N_4		
d/Å	Intensity	*d*/Å	*hkl*	Intensity
6.87	m	6.69	100	8
		4.32	101	50
3.93	m	3.88	110	30
3.42	s	3.37	200	30
		2.893	201	85
		2.823	002	6
2.76	s	2.599	102	75
2.65	m	2.547	210	100
		2.320	211	60
		2.283	112	8
2.27	w	2.244	300	6
		2.158	202	30
2.097	m	2.083	301	55
2.036	w	1.937	220	2
		1.884	212	8
		1.864	310	8
		1.806	103	12
1.796	m	1.771	311	25
		1.751	302	2
		1.637	203	8
1.634	m	1.596	222	35
		1.552	312	2
1.56	w	1.542	320	6
		1.507	213	8
		1.486	321	70
		1.437	303	55
1.469	s	1.418	411	60
		1.406	004	20
		1.376	104	12
1.354	w	1.351	322	75
		1.343	500	2
		1.321	114,313	30
		1.306	501	16
		1.299	412	50
		1.293	330	30
		1.269	420	8
1.271	m	1.238	421	30
1.234	m	1.229	214	30
		1.213	502	8

et al.[10] However, it is somewhat surprising that the lattice parameters *a* and *c* of the SiCN film are still similar to those of α-Si_3N_4 even with 20 at.% of C substitution for Si. On the other hand, we can not rule out the possibility of a crystal structure exhibiting long range order distinct from the α-Si_3N_4 structure and yet still maintaining several *d* spacings in close proximity with those of α-Si_3N_4.

3.2 Gas phase considerations

The difficulty of carbon incorporation into the films without H_2 addition could be attributed to the fact that the H_3C–H bond (438.5 kJ mol^{-1}) is much stronger than the H_3Si–H bond (384 kJ mol^{-1}).[18] Therefore, SiH_4 can be dissociated into active radicals more easily than can CH_4, leading to concentrations of active carbon species which are much less than those of active silicon species. The expressions for the rate constants of the related dissociation reactions are listed in Table 3,[19] in which two dissociation channels, r1 and r2, for SiH_4 are listed. As reported,[20] r2 dominates the SiH_4 dissociation in a dilute gas environment like our ECR reactor. Assuming that the gas temperature near the substrate surface is close to the substrate temperature, 1000 K, the rate constant of the SiH_4 dissociation reaction r2 is 10 orders of magnitudes higher than that of CH_4 r3. This explains why carbon is not detected in the film for a CH_4 : SiH_4 ratio as high as 100 : 1, as shown in Fig. 2(b). Methyl radicals cannot be produced through the reaction $CH_4 + N \rightarrow CH_3 + NH$, since the abstraction reaction is endothermic.

Table 3 The rate constant expressions of some gas phase reactions (see ref. 18)

Reaction	k	k at 1000 K
r1 $SiH_4 \rightarrow SiH_3 + H$	$3.91 \times 10^{15} \exp(-44966/T)\ s^{-1}$	$1.16 \times 10^{-4}\ s^{-1}$
r2 $SiH_4 \rightarrow SiH_2 + H_2$	$3.28 \times 10^{16} \exp(-31832/T)\ s^{-1}$	$4.91 \times 10^{2}\ s^{-1}$
r3 $CH_4 \rightarrow CH_3 + H$	$3.72 \times 10^{15} \exp(-52246/T)\ s^{-1}$	$7.59 \times 10^{-8}\ s^{-1}$
r4 $SiH_4 + H \rightarrow SiH_3 + H_2$	$1.39 \times 10^{13} \exp(-1400/T)\ cm^3\ mol^{-1}\ s^{-1}$	$3.43 \times 10^{12}\ cm^3\ mol^{-1}\ s^{-1}$
r5 $CH_4 + H \rightarrow CH_3 + H_2$	$2.25 \times 10^{4} T^3 \exp(-4406/T)\ cm^3\ mol^{-1}\ s^{-1}$	$2.75 \times 10^{11}\ cm^3\ mol^{-1}\ s^{-1}$

When H_2 is introduced into the system the H atoms produced will enhance the hydrogen abstraction reactions listed as r4 and r5 in Table 3, which are effective for the production of active carbon and silicon species at high hydrogen concentration. At a typical temperature of 1000 K, the rate constant of CH_3 formation in r5 is only one order of magnitude lower than that of SiH_3 in r4, which is drastically enhanced from the 10 orders of magnitudes difference in r2 and r3. Therefore, introducing additional hydrogen into the system provides a more efficient reaction path for the formation of active carbon species. To confirm the above argument, we apply *in situ* optical emission spectroscopy to monitor the gas phase species in the ECR plasma.

Typical OES spectra monitored *in situ* from the $N_2/CH_4/SiH_4$ ECR plasma with and without H_2 addition are shown in Fig. 5, along with the spectra of N_2, and N_2/H_2 plasma for comparison. An expanded view of the spectra between 400 and 450 nm is shown in Fig. 6. As shown in Fig. 5, the N_2 1st and 2nd positive emission bands as well as N_2^+ 1st negative emission lines are observed in all spectra.[21–23] N_2/H_2 plasma (spectrum II) shows H_α and H_β at 656.2 and 486.1 nm, respectively, indicating that hydrogen radicals are indeed formed in the N_2 plasma with H_2 addition. When both nitrogen and methane were introduced in the plasma strong emission for CN radicals at 388.3 nm was observed. This line can be ascribed to the $B^2\Sigma$–$X^2\Sigma$ transition of CN. Stronger H_α and H_β emission lines are also observed in spectrum IV than in spectrum III due to addition of H_2. Meanwhile, H_2 addition produces stronger H_γ emission at 434.0 nm, that overlaps with one of the N_2 2nd emission lines at 434.3 nm, in spectra III and IV of Fig. 6. Furthermore, the emission lines of CN (from $B^2\Sigma$–$X^2\Sigma$) at 421.6, 418.1 and 415.2 nm as well as CH (from $A^2\Delta$–$X^2\Pi$) at 431.4 nm are observed in spectra III and IV of Fig. 6. Methyl radical, acetylene, methane, and silane do not fluoresce efficiently and have not been detected using the OES technique.[21–23] Likewise, the emission lines of SiH_2 and CH_2 radicals are completely obscured by the strong emission lines of N_2 plasma.

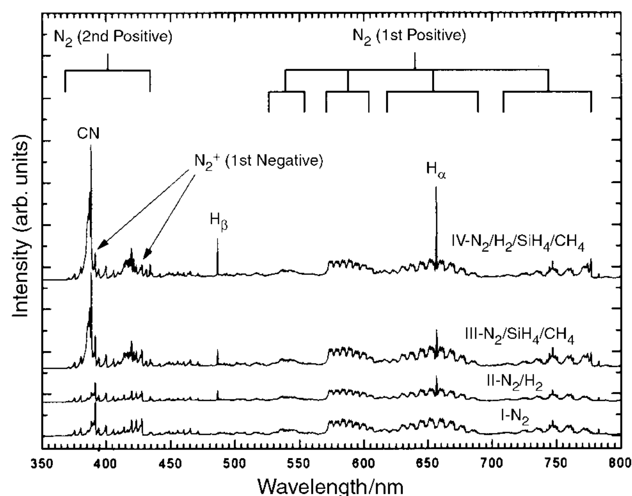

Fig. 5 Typical OES spectra of (I) N_2, (II) N_2/H_2, (III) $N_2/SiH_4/CH_4$ and (IV) $N_2/H_2/SiH_4/CH_4$ ECR plasmas in the range of 350–800 nm.

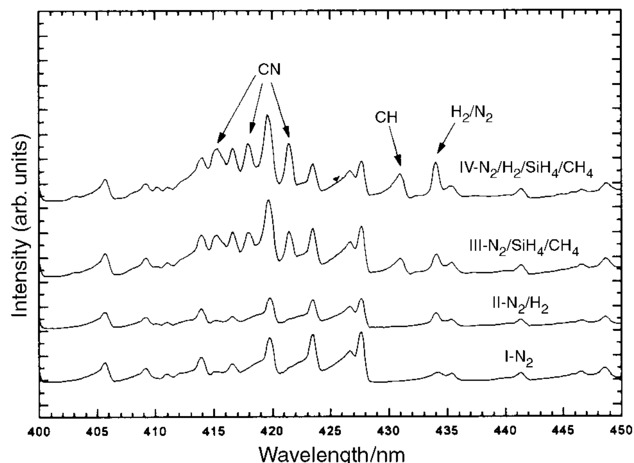

Fig. 6 Expanded view of the OES spectra of (I) N_2, (II) N_2/H_2, (III) $N_2/SiH_4/CH_4$ and (IV) $N_2/H_2/SiH_4/CH_4$ ECR plasmas in the range of 400–450 nm.

Comparing spectra III and IV in Fig. 6, substantial increases in the emission of the CH line at 431.4 nm and the CN lines at 388.3, 421.6, 418.1 and 415.2 nm were observed when additional hydrogen was introduced. The signal intensity is related to the population of the CH/CN excited states, which may be directly proportional to the gas phase concentration of the CH/CN radicals ignoring non-radiative relaxation such as quenching in the gas phase. The increase of CH/CN emission lines, qualitatively interpreted as an increase of the CH/CN radical concentration, can be attributed to the abstraction reaction r5 in Table 3. The addition of H enhances the production of methyl radicals, and therefore further enhances the CH and CN radical concentrations. While the CH radical detected in the OES spectra is reactive and can be directly related to film growth, CN, however, is a triple-bond radical and is unlikely to participate in film growth. Nevertheless, the increase in either one of them is indirect evidence for the increase of active carbon species in the system, which may correlate with an increase of the carbon content in the film. Therefore, from film stoichiometry as well as OES evidence, we conclude that hydrogen addition to the system enhances carbon incorporation in the film through the abstraction reactions shown in Table 3.

Furthermore, as shown in Table 1, not only the H_2 addition is necessary for carbon incorporation, the concentration of methane in the gas phase also affects the resultant composition of the film. As known in diamond growth by CVD, high $H:C_xH_y$ ratios do not favor carbon deposition due to preferential etching of surface-bonded carbons by hydrogen atoms.[12] Moreover, surface-bonded carbons could also be sputtered chemically by N_2^+ ions to form CN radicals or C_2N_2 molecules.[24] Therefore, a certain methane concentration is required for the carbon deposition rate to overcome the carbon etching rate by H atoms and N_2^+ ions. This explains why there is no carbon incorporation in the film for $CH_4:SiH_4$ ratio below 100 : 1.

4 Conclusion

Hydrogen plays a key role in the growth of SiCN film by the ECR plasma CVD method. Without additional hydrogen, no carbon incorporation can be found in the deposited films. Adding H_2 to the system effectively enhances active carbon species in the gas phase, which is predicted by consideration of likely gas phase reactions and also confirmed by *in situ* OES spectra. These observations suggest a route to improvement in carbon composition control as well as high quality SiCN film growth in the future.

Acknowledgements

The authors would like to thank Dr. K. P. Liu for helpful discussion in OES interpretation and X.-J. Guo for assistance in TEM analysis. The financial support of this work by the National Science Council in Taiwan, No. NSC 88-2112-M-001-032 and NSC 88-2112-M-002-022, is gratefully acknowledged.

References

1 G. Sato, E. C. Samano, R. Machorro and L. Cota, *J. Vac. Sci. Technol. A*, 1998, **16**, 1311.
2 F. J. Gomez, P. Prieto, E. Elizalde and J. Piqueras, *Appl. Phys. Lett.*, 1996, **69**, 773.
3 R. Giorgi, S. Turtu, G. Zappa, E. Borsella, S. Botti, M. C. Cesile and S. Maartelli, *Appl. Surf. Sci.*, 1996, **93**, 101.
4 G. Viera, J. L. Andujar, S. N. Sharma and E. Bertran, *Diamond Relat. Mater.*, 1998, **7**, 407.
5 R. Riedel, A. Greiner, G. Miehe, W. Dressler, H. Fuess, J. Bill and F. Aldinger, *Angew. Chem., Int. Ed. Engl.*, 1997, **36**, 603.
6 L. C. Chen, C. Y. Yang, D. M. Bhusari, K. H. Chen, M. C. Lin, J. C. Lin and T. J. Chuang, *Diamond Relat. Mater.*, 1996, **5**, 514.
7 D. M. Bhusari, C. K. Chen, K. H. Chen, T. J. Chuang, L. C. Chen and M. C. Lin, *J. Mater. Res.*, 1997, **12**, 322.
8 L. C. Chen, D. M. Bhusari, C. Y. Yang, K. H. Chen, T. J. Chuang, M. C. Lin, C. K. Chen and Y. F. Huang, *Thin Solid Films*, 1997, **303**, 66.
9 L. C. Chen, C. K. Chen, S. L. Wei, D. M. Bhusari, K. H. Chen, Y. F. Chen, Y. C. Jong and Y. S. Huang, *Appl. Phys. Lett.*, 1998, **72**, 2463.
10 A. Badzian, T. Badzian, W. D. Drawl and R. Roy, *Diamond Relat. Mater.*, 1998, **7**, 1519.
11 K. H. ChenJ.-J. Wu, C. Y. Wen, L. C. Chen, C.-W. Fan, P.-F. Kuo, Y.-F. Chen, Y.-S. Huang, *Thin Solid Films*, 1999, **355–356**, 205.
12 K. E. Spear and J. P. Dismukes, *Synthetic Diamond: Emerging CVD Science and Technology*, John Wiley & Sons, Pennington, NJ, 1994.
13 Y. Zhang, Z. Zhou and H. Li, *Appl. Phys. Lett.*, 1996, **68**, 634.
14 Y. Chen, L. Guo, F. Chen and E. G. Wang, *J. Phys.: Condensed Matter*, 1996, **8**, L685.
15 Y. Feng, Z. Zhou, Y. Zhou and G. Zhao, *Nucl. Instrum. Methods B*, 1994, **86**, 225.
16 Y. Feng, Z. Zhou. G. Zhao and F. Yang, *Nucl. Instrum. Methods B*, 1994, **94**, 11.
17 D. Marton, K. J. Boyd, A. H. Al-Bayati, S. S. Todorov and J. W. Rabalais, *Phys. Rev. Lett.*, 1994, **73**, 118.
18 D. R. Lide, *CRC Handbook of Chemistry and Physics*, 76th edn., CRC Press, Boca Raton, FL, 1995.
19 F. Westly, D. H. Frizzell, J. T. Herron, R. F. Hampson and W. G. Mallard, NIST Chemical Kinetics Database, Version 6.01, US Department of Commerce, Technology Administration, National Institute of Standards and Technology, Standard Reference Data Program, Gaithersburg, MD, 1994.
20 G. Turban, *Pure Appl. Chem.*, 1984, **56**, 215.
21 R. Pearse and A. Gaydon, *The identification of molecular spectra*, John Wiley & Sons, New York, 1976.
22 G. Herzberg, *Molecular spectra and molecular structure I. Spectra of diatomic molecules*, Van Nostrand Reinhold, New York, 1950.
23 G. Herzberg, *The spectra and structures of simple free radicals*, Vail-Ballou Press, Ithaca, NY, 1971.
24 P. Hammer and W. Gissler, *Diamond Relat. Mater.*, 1996, **5**, 1152.

Paper a908523h